

Article

Basalt-Fiber-Reinforced Phosphorus Building Gypsum Composite Materials (BRPGCs): An Analysis on Their Working Performance and Mechanical Properties

Lei Wu ^{1,2} , Zhong Tao ^{1,2,*}, Ronggui Huang ^{1,2}, Zhiqi Zhang ^{1,2}, Jinjin Shen ^{1,2} and Weijie Xu ^{1,2}

¹ Faculty of Civil Engineering and Mechanics, Kunming University of Science and Technology, Kunming 650599, China; wulei0324@stu.kust.edu.cn (L.W.); 20212210030@stu.kust.edu.cn (R.H.)

² Yunnan Seismic Engineering Technology Research Center, Kunming University of Science and Technology, Kunming 650500, China

* Correspondence: taozhong@kust.edu.cn

Abstract: The preparation of fiber-reinforced phosphorus building gypsum composite materials (FRPGCs) is an important approach to enlarge the utilization of phosphogypsum resources. Through reinforcing phosphorus building gypsum (PBG) with basalt fiber (BF), this article probes into the effects of the length and fiber content of BF on the working performance and mechanical properties of basalt-fiber-reinforced phosphorus building gypsum composite materials (BRPGCs) and accesses the toughness of BRPGCs under bending loads using residual strength. The results showed that the addition of BF could significantly promote the mechanical properties of BRPGCs. However, due to the adverse effect of fibers on the working performance of BRPGCs, the fiber content was constrained. After adding 1.2% of 6 mm BF, the bending strength and compressive strength of FRPGCs reached maximum values of 10.98 MPa and 29.83 MPa, respectively. Under a bending load, BRPGCs exhibited an apparent ductile behavior. The P- δ curve presented five stages, with an evident phase of strength stability after cracking. A larger fiber content was conducive to the toughness of BRPGCs. When 1.6% of 6 mm BF was added, the residual strength of FRPGCs could reach 6.77 MPa.

Keywords: basalt fiber; phosphorus building gypsum; working performance; mechanical properties; load deformation curve



Citation: Wu, L.; Tao, Z.; Huang, R.; Zhang, Z.; Shen, J.; Xu, W.

Basalt-Fiber-Reinforced Phosphorus Building Gypsum Composite Materials (BRPGCs): An Analysis on Their Working Performance and Mechanical Properties. *Inorganics* **2023**, *11*, 254. <https://doi.org/10.3390/inorganics11060254>

Academic Editors: Roberto Nisticò, Torben R. Jensen, Luciano Carlos, Hicham Idriss and Eleonora Aneggi

Received: 5 May 2023

Revised: 7 June 2023

Accepted: 8 June 2023

Published: 9 June 2023



Copyright: © 2023 by the authors. Licensee MDPI, Basel, Switzerland. This article is an open access article distributed under the terms and conditions of the Creative Commons Attribution (CC BY) license (<https://creativecommons.org/licenses/by/4.0/>).

1. Introduction

Phosphogypsum is a solid waste produced by the phosphate chemical industry that can cause soil and water pollution [1,2]. Disposing large amounts of newly generated and stockpiled phosphogypsum is a global challenge [3,4]. This problem is especially severe in China, where more than 500 million tons of phosphogypsum are currently stockpiled and more than 55 million tons of phosphogypsum are generated each year, with a recycling rate of only 40% [5,6]. One important way to recycle phosphogypsum is by preparing phosphorus building gypsum, but its use is limited due to inferior properties compared with cement or natural building gypsum [7,8]. Thus, improving the performance of PBG is a critical research task. The widespread use of PBG can promote the resource utilization of phosphogypsum and help reduce carbon emissions in the construction industry as a low-carbon building material [9].

In contrast with gypsum, fiber-reinforced gypsum composite materials (FRGCs) have better mechanical properties and can be used as paperless gypsum boards, gypsum planks, and molded gypsum [10,11]. Fibers such as polyvinyl alcohol fiber (PVA), polypropylene fiber (PP), and glass fiber are usually adopted to enhance the performance of gypsum [12]. Gonçalves et al. [13] evaluated the feasibility of utilizing recycled glass fibers for the preparation of FRGCs. After adding 6 wt% of recycled glass fibers, the bending strength of FRGCs could increase by 66%. Suarez [14] adopted three polymeric fibers to prepare

FRGCs and explored the influence law of fiber length on the fracture performance of FRGCs. Cong [15] prepared FRGCs using PP and PVA and made a thorough evaluation of the processability, bending properties, and toughness of FRGCs.

With the advantages of a low cost, excellent mechanical properties, and good fire resistance, basalt fiber (BF) has a great application potential in the field of building materials [16,17]. Li [18] treated BF with HCl, NaOH, and silane coupling agents, respectively, and analyzed the effects of the three treatment methods as well as fiber length and fiber content on the performance of BF-reinforced natural building gypsum composite materials (BFRGs). An appropriate fiber content can promote the bending strength of BFRGs by more than 50%. Meanwhile, Li [19] studied the effects of the dispersion mode of fibers on the working performance and mechanical properties of BFRGs. The bending strength of BFRGs prepared by the premix method increased by 40.6%. However, there was a decrease in compressive strength. Xie [20] used BF to reinforce desulfurized building gypsum and probed into the effects of BF on the working performance and mechanical properties of desulfurized building gypsum. Under the conditions of a fiber length of 9 mm and a fiber content of 0.7%, the bending strength of the composite material was significantly improved. Given the successful application of BF in reinforcing natural building gypsum and desulfurized building gypsum, BF may be used to improve the mechanical properties of phosphorus building gypsum. Wu [21] studied the effects of BF on the bending strength of phosphorus building gypsum. However, the effects of the fiber dosage and length on the working performance and bending toughness of basalt-fiber-reinforced phosphorus building gypsum composite materials (BRPGCs) were not involved.

To synthetically investigate the influence of BF on the working performance and mechanical properties of BRPGCs, two lengths of BF—6 mm and 12 mm—were adopted in this paper. The effects of fiber length and fiber addition on the fluidity and setting time of slurry from BRPGCs as well as the bending strength, bending toughness, and compressive strength of BRPGCs were explored through experiments. The fracture behavior of BRPGCs was analyzed through the P - δ curve. The mechanism of the influence of fibers on the performance of BRPGCs was preliminarily analyzed. This paper provides an essential research basis for the further application of BRPGCs.

2. Results and Discussion

2.1. Working Performance

2.1.1. Fluidity

The addition of BF caused a significant alteration in the fluidity of the slurry from BRPGCs, as shown in Figure 1. As the fiber content increased, the fluidity of the slurry from BRPGCs gradually decreased. For the 6 mm BF, when the fiber content reached 2%, the fluidity of the slurry from BRPGCs was lost and was remarked as fluidity of 60 mm. For the 12 mm BF, when the fiber content reached 1.6%, the slurry from BRPGCs lost its fluidity. With the same BF addition, the influence of the 6 mm BF on the fluidity of the slurry from BRPGCs was less than that of the 12 mm BF. This result was similar to the research on FRGCs, but the influence of BF on fluidity was greater than that of PP [15,18–20].

This phenomenon agreed with observations in other FRGCs [12,15]. When BF was added to the slurry of phosphorus building gypsum, the large surface area of the fibers partially adsorbed water, the water films on the surfaces of solid substances in the slurry became thinner, and resistance to particle movement increased, thus lowering the fluidity of the slurry. Meanwhile, fibers distributed in the slurry formed a grid structure, which impeded the flow of the slurry. Longer fibers and larger additions would strengthen this grid effect, leading to a greater decrease in the fluidity of the slurry.

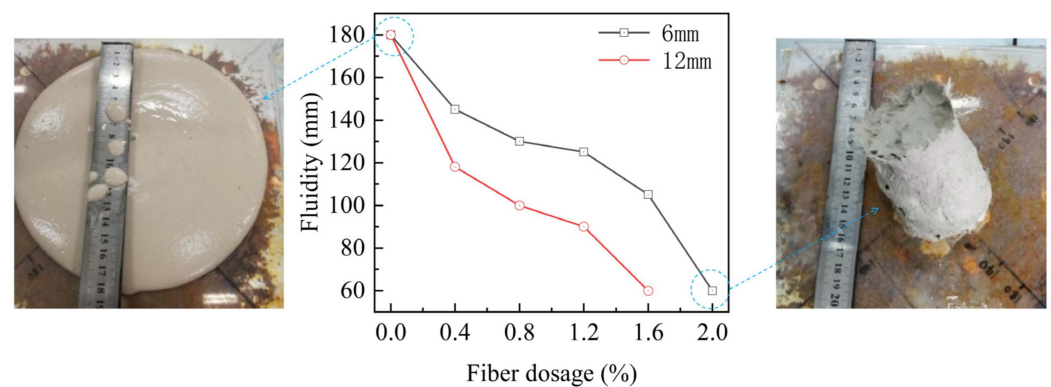


Figure 1. Influence of BF on the fluidity of the slurry from BRPGCs.

2.1.2. Setting Time

The addition of BF shortened the setting time of the slurry from BRPGCs, as shown in Figure 2. For the 6 mm BF, when the fiber content reached 1.6%, the initial setting time of the slurry from BRPGCs in the blank group decreased from 13 min and 20 s to 10 min and 10 s; the final setting time reduced from 30 min and 10 s to 25 min and 30 s. For the 12 mm BF, when the fiber content reached 1.2%, the initial setting time of the slurry from BRPGCs lessened to 10 min and 30 s and the final setting time decreased to 25 min and 10 s. On the whole, with the same addition, the fiber length hardly affected the setting time of the slurry from BRPGCs. This result was widely observed and was consistent with research on FRGCs [15,18–20].

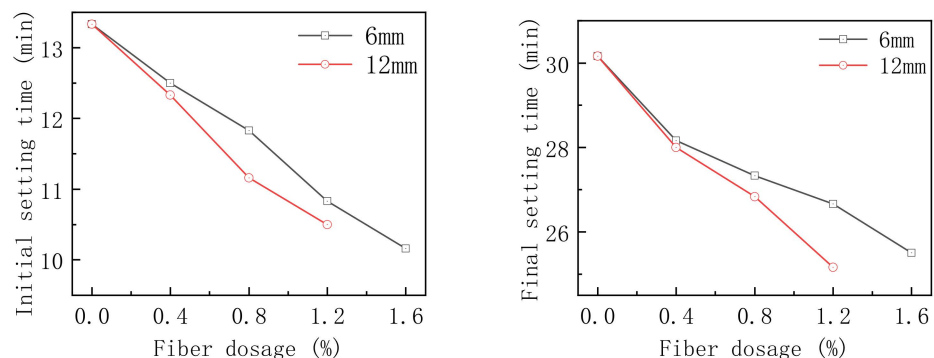


Figure 2. Influence of BF on the setting time of the slurry from BRPGCs.

Adding BF enlarged the total surface area of solid substances in the slurry from BRPGCs, thinned the water films on the surfaces of gypsum particles, narrowed the particle spacing, and accelerated the hydration reaction. Therefore, the setting time of the slurry from BRPGCs was shortened. The increase in the fiber surface area of composite materials was mainly relevant to the volume fraction of fibers, which were scarcely affected by fiber length. Therefore, the influence of fiber length on the setting time of the composite slurry was minimal.

2.2. Mechanical Properties

2.2.1. Analysis of P- δ Curve

During bending loading, the P- δ curve of BRPGCs had an apparent consistency. After cracking, BRPGCs possessed a certain residual bearing capacity, as shown in Figure 3. The load curve showed that the addition of BF greatly increased the peak load of BRPGCs. BRPGCs exhibited significant toughness after cracking and the residual strength also varied with changes in fiber length and fiber addition. The specific behavior is discussed in Sections 2.2.2 and 2.2.3.

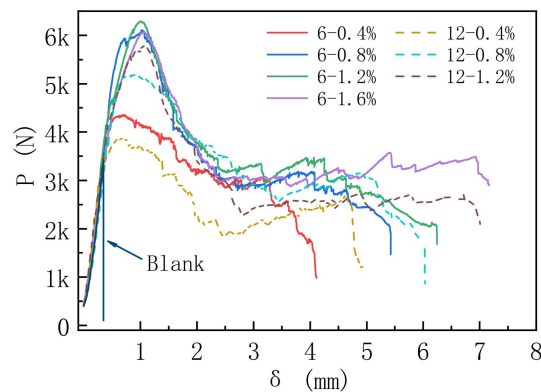


Figure 3. The P- δ curve of BRPGCs in the bending test.

The bending fracture behavior of BRPGCs can be summarized into five typical stages, as shown in Figure 4. The first stage (O–A) was the elastic phase, displaying elastic deformation. The phosphorus building gypsum matrix and BF were subjected to joint forces. The second stage (A–B) was the lifting phase. Due to the brittle feature of the phosphorus building gypsum matrix, the matrix cracked first. The crack did not rapidly expand, owing to the bridging effect of the fibers. The BF at the crack underwent elastic deformation under stresses. The bearing capacity of BRPGCs continued to increase until the peak point B. The third stage (B–C) was the declining phase. As the load continued to increase, the crack opening enlarged and BF at the crack began to pull out. The bearing capacity of BRPGCs decreased. The crack rapidly expanded, with more BF participating in bridging the crack. The fourth stage (C–D) was the stable phase. As the crack expanded, more and more BF bridged the crack. During pullout, the fibers at the opening of the crack dissipated energy through the interface as friction behavior between the fibers and the matrix. The fibers at the pointed ends of the crack showed elastic deformation and provided a bearing capacity. At this stage, the bearing capacity of BRPGCs was stable, with a slight decrease. The fifth stage (D–E) was the failure phase. With the continuous expansion of the crack, the fibers at the opening of the crack started to pull out and were no longer able to provide a bearing capacity. The bearing capacity of BRPGCs dropped sharply until complete failure.

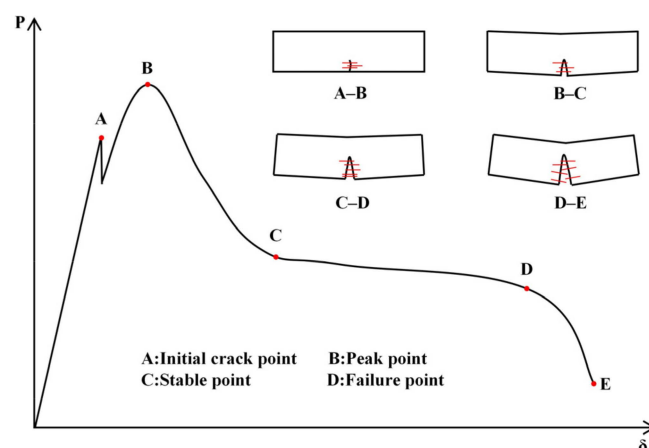


Figure 4. The typical P- δ curve of BRPGCs.

2.2.2. Bending Strength

The addition of BF had a significant impact on the bending strength of BRPGCs, as shown in Figure 5. The bending strength of BRPGCs increased with the fiber content. When the content of 6 mm BF reached 1.2%, the oven-dry bending strength of BRPGCs was up to the peak value of 12.14 MPa, 85.4% higher than the blank group. However, further

increasing the fiber content caused a decrease in the bending strength of BRPGCs. This was mainly because when the fiber content was exceptionally high, the fluidity of the slurry from BRPGCs was quite low and a large number of pores appeared during the forming of BRPGCs, resulting in a decrease in the strength of the matrix. When the content of the 12 mm BF was added to 1.2%, the oven-dry bending strength of BRPGCs reached the maximum of 10.98 MPa, 67.7% higher than that of the blank group. With the same fiber addition, the reinforcement effect of the 6 mm BF was better than the 12 mm BF, which was also due to more defects generated by the 12 mm BF during the forming process of BRPGCs. Compared with other studies of FRGCs, the bending strength improvement of BRPGCs in this paper was more significant (see Table 1).

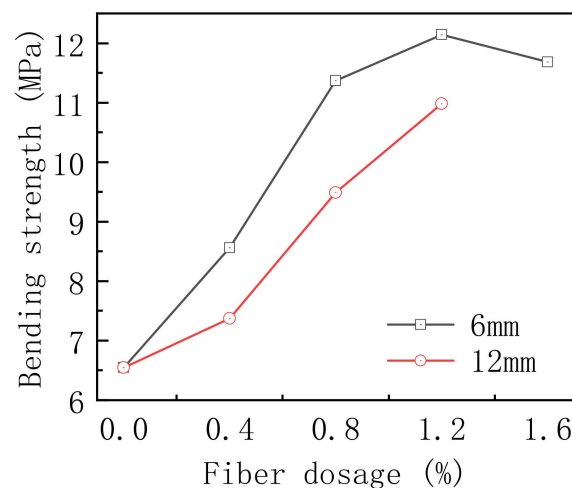


Figure 5. The effect of BF on the oven-dry bending strength of BRPGCs.

Table 1. Performance comparison with other research results.

	Fiber	Bending Strength/Flexural Strength	Compressive Strength
This paper	6 mm, 17.4 μm , and 1.2% BF	Increased by 85.4%	Increased by 69%
Gonçalves [13]	10 mm; 6 wt% E-glass fiber	Increased by 66%	-
Suarez [14]	12 mm, 31 μm , and 10 Kg/m ³	-	Decreased by 6.7%
Cong [15]	12 mm, 12 μm , and 1.2% PVA	Increased by 48%	Decreased by 6.6%
Li [18]	10 mm; 10% PVA	Increased by 78.3%	-
Li [19]	10 mm, 13 μm , and 0.5% BF	Increased by 40.6%	Decreased by 11.1%
Xie [20]	6 mm, 17 μm , and 0.7 wt% BF	Increased by 36.53%	Increased by 10.31%

2.2.3. Bending Toughness

The residual strength of BRPGCs was calculated according to the P- δ curve obtained in the bending test of BRPGCs, and the result is shown in Figure 6. It could be seen that the residual strength of BRPGCs increased with the fiber content, exhibiting a better toughness performance. The reason may be that when the fiber content was higher, after BRPGCs cracked, more fibers were distributed at the crack and provided a better bridging effect. However, the rise in fiber length had adverse effects on the residual bending strength of BRPGCs. It was mainly because the addition of 12 mm BF negatively affected the strength of BRPGCs and resulted in more defects in BRPGCs, which accelerated the expansion of the crack in the bending test. Expressing the contribution of the 12 mm BF to the toughness of BRPGCs solely through residual strength is still not comprehensive. From Figure 1, we could see that although the 12 mm BF had slight effects on peak load and residual strength, with the same addition, BRPGCs with 12 mm BF achieved greater ultimate deformation and exhibited a better deformation ability. This was because the 6 mm BF was easier to completely pull out from the matrix; in comparison, the 12 mm BF had a larger extraction length during the production process, resulting in a better energy dissipation capacity.

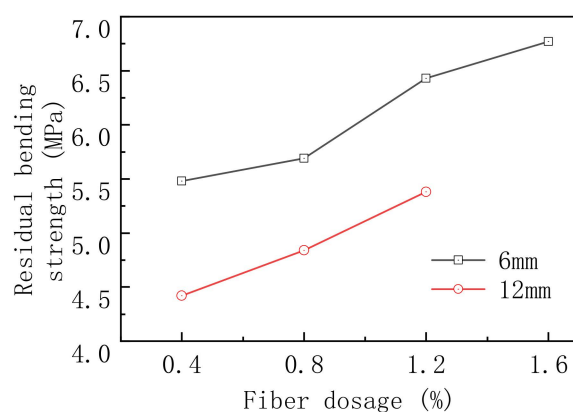


Figure 6. The influence of BF on the residual strength of BRPGCs.

When observing the micromorphology of BRPGCs after fracture through SEM, it could be seen that there was no significant plastic deformation of the BF during the fracture of BRPGCs, indicating that the BF was not a factor that consumed the energy of the fracture during the fracture. After being pulled out, BF left smooth marks and the interface between the hydration products of PBG and BF was neat. It could be inferred that BF and PBG hydration products did not form chemical coupling, but were combined through mechanical coupling. During the fracture process of BRPGCs, the energy of the fracture was mainly dissipated through sliding and friction between the BF and hydration products (see Figure 7).

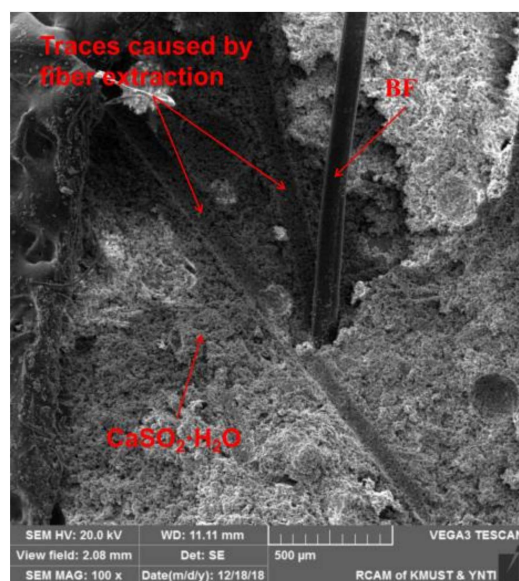


Figure 7. Microstructure of BRPGC.

2.2.4. Compressive Strength

The oven-dry compressive strength of BRPGCs remarkably increased with the addition of BF, as shown in Figure 8. Overall, the compressive strength of BRPGCs was enhanced with the fiber content. However, an excessive fiber content also caused a decrease in strength. When the content of 6 mm BF was 1.2%, the compressive strength of BRPGCs reached the maximum value of 29.83 MPa, 69.0% higher than that of the blank group. When the content of 12 mm BF was 1.2%, the compressive strength of BRPGCs reached a maximum value of 27.33 MPa, 54.8% higher than that of the blank group. With the same fiber content, the reinforcement effect of 6 mm BF was superior to that of 12 mm BF. Compared with other studies of FRGCs, the compressive strength improvement of BRPGCs in this paper was more significant (see Table 1).

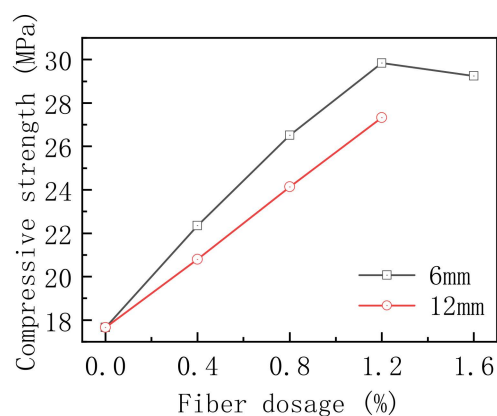


Figure 8. The impact of BF on the oven-dry compressive strength of BRPGCs.

As the elastic modulus of BF was much higher than that of phosphorus building gypsum, the addition of BF promoted the elastic modulus of BRPGCs. Under the action of a compressive load, a higher elastic modulus could lessen the transverse deformation of BRPGCs and delay material failure, thus enhancing the compressive strength of BRPGCs. The adverse effects of a larger fiber content and length on the compressive strength of composite materials were chiefly due to the defects in BRPGCs and the decrease in matrix strength during the forming process caused by the decline in the fluidity of the slurry from BRPGCs.

3. Materials and Methods

3.1. Raw Materials

The phosphogypsum used in this study was provided by Yunnan Yuntianhua Co., Ltd. (Kunming, China). After being washed in the laboratory to remove impurities, it was then calcined at 145 °C for 6 h to prepare phosphorus building gypsum (light yellow powders), as shown in Figure 9. Its chemical compositions are shown in Table 2. The XRD analysis of PBG is shown in Figure 10.



Figure 9. Phosphorus building gypsum.

Table 2. Chemical compositions of phosphogypsum.

Component	SiO ₂	Al ₂ O ₃	Fe ₂ O ₃	MnO	MgO	CaO	K ₂ O	P ₂ O ₅	SO ₃	Organism
Content (%)	14.52	1.66	0.15	0.005	0.17	31.94	0.22	0.94	45.38	0.25

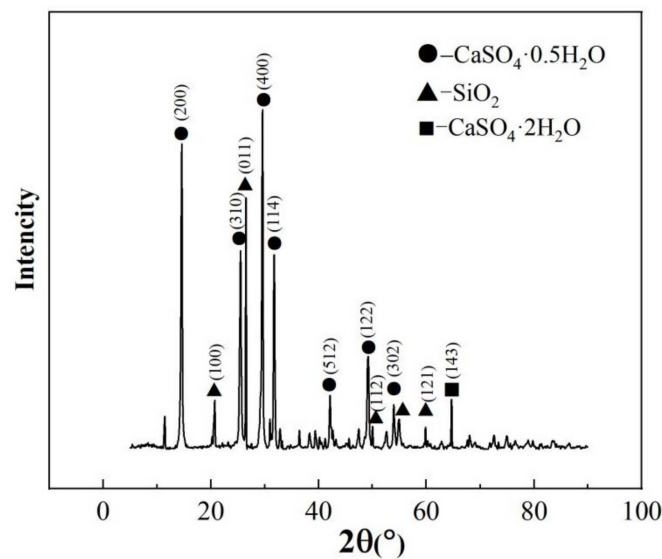


Figure 10. Results of XRD analysis.

BF was produced by Shanghai Chenqi Chemical Technology Co., Ltd., Shanghai, China, in the shape of bronze-colored coarse sand, as shown in Figure 11. The specifications adopted in this article were 6 mm- and 12 mm-long chopped sand. The physical properties are shown in Table 3.



Figure 11. Basalt fiber.

Table 3. Physical properties of BF.

Density	Tensile Strength	Elongation Rate	Maximum Working Temperature	Diameter	Tensile Modulus of Elasticity
2.65 g/cm	≥2000 MPa	≥2.5%	650 °C	17.4 μm	100 GPa

The water reducer used in this experiment was a polycarboxylic-acid-type water reducer prepared in the laboratory and was a light yellow oily liquid with a solid content of 40%.

3.2. Experiment Design

For the blank group in the experiment, the mixture ratio was 1200 g phosphorus building gypsum, 6 g water reducer, and 370 g water; the fluidity was 180 mm. The volume fractions for the BF of each length were 0.4%, 0.8%, 1.2%, 1.6%, and 2.0% (see Table 4). When the fluidity of the composite slurry could not be tested, the fiber content no longer increased. When the fluidity of the experimental group was unable to be tested, indicators such as the fluidity and mechanical properties stopped being tested.

Table 4. Mix proportions.

No.	PBG/g	Water Reducer/g	Water/g	Length of BF/mm	Volume Fractions for BF/%
1	1200	6	370	-	-
2	1200	6	370	6	0.4
3	1200	6	370	6	0.8
4	1200	6	370	6	1.2
5	1200	6	370	6	1.6
6	1200	6	370	6	2.0
7	1200	6	370	12	0.4
8	1200	6	370	12	0.8
9	1200	6	370	12	1.2
10	1200	6	370	12	1.6

3.3. Experiment Methods

3.3.1. Working Performance

The fluidity and setting time of the slurry from BRPGCs were primarily determined indicators and referred to the “Determination of Physical Properties of Building Gypsum Net Slurry”. (GB/T 17669.4-1999) Chinese national standard [22].

The flow spread of different groups of PBG was tested using a cylinder with specifications of $\varphi 50 \times 50$ mm. According to the mix proportions for the PBG plaster in Section 3.2, BF was added to the water and stirred until homogeneous. The PBG was then added and mixed for 60 s to obtain the plaster. The plaster was quickly poured into a clean, moist cylinder and excess plaster was scraped off. The cylinder was lifted to measure the vertical diameter of the disk formed by the expansion of the PBG plaster and calculate the average value as the flow spread of the test group.

The setting time was assessed using Vicat apparatus. The initial setting time was the time when the needle did not touch the glass floor and the final setting time was the time when the depth of the needle inserted into the slurry was not greater than 1 mm.

3.3.2. Mechanical Properties

The specification of the specimen of BRPGCs used for mechanical property testing was $40 \text{ mm} \times 40 \text{ mm} \times 160 \text{ mm}$. After forming, the specimen was naturally cured for 24 h and dried to a constant weight at 40 ± 4 °C. A microcomputer-controlled universal material testing machine was used for four-point bend loading, as shown in Figure 12. The P- δ curve of the specimen was collected. Displacement control was adopted in the loading process, with a loading rate of 0.5 mm/min and a sampling frequency of 10 Hz.

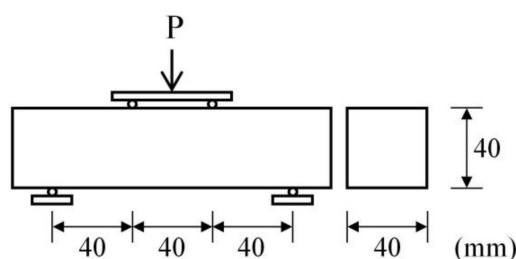


Figure 12. Schematic diagram of the test of four-point bend loading.

According to the obtained bending P- δ curve, the peak load of the curve was regarded as the maximum load (P) of the specimen. The flexural strength (R_f) of the specimen was obtained by the following equation:

$$R_f = PL/bh^2$$

where P represents the maximum load, L denotes the span of the specimen, and b and h are the width and height of the specimen, respectively.

The bending toughness was evaluated using the residual strength method [23], as shown in Figure 13. The deformation corresponding with the peak load of the P- δ curve was remarked as δ . Loads of P1, P2, P3, P4, and P5 corresponding with deformations of 1.5 δ , 2 δ , 3 δ , 4 δ , and 5 δ were found, respectively. Due to the remarkable fluctuation in the bearing capacity of BRPGCs after cracking, the average value of the load in the range of [-0.005 mm, 0.005 mm] before and after the corresponding deformation was taken as the load, as shown in Figure 13.

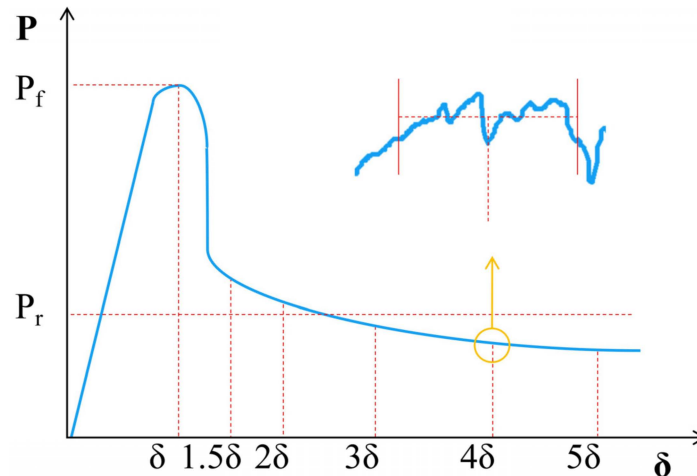


Figure 13. Schematic diagram of the calculation of bending toughness.

The residual load (P_r) was obtained by the following equation:

$$P_r = \frac{\alpha_1 P_1 + \alpha_2 P_2 + \alpha_3 P_3 + \alpha_4 P_4 + \alpha_5 P_5}{\alpha_1 + \alpha_2 + \alpha_3 + \alpha_4 + \alpha_5}$$

where α_1 , α_2 , α_3 , α_4 , and α_5 are weighted coefficients; the values were 0.25, 0.50, 0.75, 1, and 1, respectively.

The residual strength (R_r) could be obtained by the following equation:

$$R_r = P_r L / bh^2$$

Three half-cut parts from different specimens after the bending test were used for the test of compressive strength. A microcomputer-controlled universal material testing machine was adopted for loading through displacement control, with a loading rate of 0.5 mm/min and a sampling frequency of 10 Hz. We recorded the maximum compressive load (P_c) and calculated the flexural strength of the specimen as follows:

$$R_c = P_c / S$$

where P_c represents the maximum compressive load in units of N and S denotes the compression area of the specimen, with a value of 40 mm \times 40 mm.

4. Conclusions

This article explored the influence law of the length and addition of BF on the working performance and mechanical properties of BRPGCs, emphasizing the fracture behavior of BRPGCs in a bending test and evaluating the bending toughness of BRPGCs through residual strength. The following conclusions were drawn:

- (1) The addition of BF had a negative impact on the working performance of the slurry from BRPGCs. As the fiber content and length increased, the fluidity of the slurry from BRPGCs decreased and the setting time shortened.

- (2) Adding BF significantly improved the mechanical properties of BRPGCs. With the increase in fiber content, the bending strength and compressive strength of BRPGCs were markedly promoted. However, the increase in fiber length had adverse effects on the mechanical properties of BRPGCs. When adding 1.2% of 6 mm BF, the bending strength and compressive strength of BRPGCs reached the maximum values of 10.98 MPa and 29.83 MPa, 67.7% and 69.0% higher than the blank group, respectively.
- (3) The P- δ curve of BRPGCs exhibited a typical characteristic of five stages. BRPGCs could reserve a good residual strength after cracking. As the fiber content increased, the toughness of the composite material increased. When 1.6% of 6 mm BF was added, the residual strength of FRPGCs reached the maximum value of 6.77 MPa.

Supplementary Materials: The following supporting information can be downloaded at: <https://www.mdpi.com/article/10.3390/inorganics11060254/s1>.

Author Contributions: Conceptualization, L.W. and Z.T.; Data Curation, R.H. and Z.Z.; Investigation, R.H.; Methodology, L.W.; Project Administration, Z.T.; Validation, J.S. and W.X.; Writing—Original Draft, L.W. and Z.Z.; Writing—Review and Editing, Z.T. All authors have read and agreed to the published version of the manuscript.

Funding: This work was supported by the Industrial High-Tech Project of the Yunnan Provincial Department of Science and Technology (202003AA080032) and the Analysis and Testing Foundations of KMUST (2021P20201110001).

Data Availability Statement: The data presented in this study are available in Supplementary Material here.

Conflicts of Interest: The authors declare no conflict of interest.

References

1. Francisco, M.; Rafael, P.; Carlos, R.C.; Sergio, C.; Pablo, C. Environmental Assessment and Management of Phosphogypsum According to European and United States of America Regulations. *Procedia Earth Planet. Sci.* **2017**, *17*, 666–669.
2. Qiang, W.; Shiyu, Z.; Ruiquan, J. An Investigation On the Anti-Water Properties of Phosphorus Building Gypsum (Pbg)-Based Mortar. *J. Therm. Anal. Calorim.* **2019**, *136*, 1575–1585.
3. Zhou, Y.; Zheng, G.; Liu, Z.; Liu, R.; Tao, C. Multi-Stage Precipitation for the Eco-Friendly Treatment of Phosphogypsum Leachates Using Hybrid Alkaline Reagents. *J. Water Process. Eng.* **2023**, *53*, 103626. [[CrossRef](#)]
4. Ignacio, V.F.; Viktoras, D.; Danutė, V.; Dalia, N. The Investigation of Phosphogypsum Specimens Processed by Press-Forming Method. *Waste Biomass Valorization* **2020**, *12*, 1539–1551.
5. Shuhua, L.; Peipei, F.; Jun, R.; Shefeng, L. Application of Lime Neutralised Phosphogypsum in Supersulfated Cement. *J. Clean Prod.* **2020**, *272*, 122660.
6. Wu, H.; Han, C.N.; Tan, Y. Research progress on reutilization of phosphogypsum on China. *Mod. Chem. Ind.* **2023**, *43*, 18–21.
7. Qiang, W.; Ruiquan, J. A Novel Gypsum-Based Self-Leveling Mortar Produced by Phosphorus Building Gypsum. *Constr. Build. Mater.* **2019**, *226*, 11–20.
8. Huang, W.; Tan, Y.; Ming, H.; Li, H.; Wu, J.; Wu, C.; Hu, B. A Novel Method for Preparing Phosphorus Building Gypsum (Pbg)-Based Building Materials with Low Water/Gypsum Ratios. *J. Mater. Cycles Waste Manag.* **2023**, *25*, 1035–1049. [[CrossRef](#)]
9. Qin, X.; Cao, Y.; Guan, H.; Hu, Q.; Liu, Z.; Xu, J.; Hu, B.; Zhang, Z.; Luo, R. Resource Utilization and Development of Phosphogypsum-Based Materials in Civil Engineering. *J. Clean Prod.* **2023**, *387*, 135858. [[CrossRef](#)]
10. Philip, C.; Sivakumar, P.; Devdas, M.; Meher, P.A. Comparative Study of Embodied Energy of Affordable Houses Made Using Gfrg and Conventional Building Technologies in India. *Energy Build.* **2020**, *223*, 110138.
11. Jun, Z.; Xiaoqian, L.; Yu, Z.; Zhu, S.; Yanxin, W.; Yi, Z.; Xiang, S. Preparation of Paper-Free and Fiber-Free Plasterboard with High Strength Using Phosphogypsum. *Constr. Build. Mater.* **2020**, *243*, 118091.
12. Jia, R.; Wang, Q.; Feng, P. A Comprehensive Overview of Fibre-Reinforced Gypsum-Based Composites (Frgcs) in the Construction Field. *Compos. Part B* **2021**, *205*, 108540. [[CrossRef](#)]
13. Gonçalves, R.M.; Martinho, A.; Oliveira, J.P. Evaluating the Potential Use of Recycled Glass Fibers for the Development of Gypsum-Based Composites. *Constr. Build. Mater.* **2022**, *321*, 126320. [[CrossRef](#)]
14. Suárez, F.; Felipe-Sesé, L.; Díaz, F.A.; Gálvez, J.C.; Alberti, M.G. On the Fracture Behaviour of Fibre-Reinforced Gypsum Using Micro and Macro Polymer Fibres. *Constr. Build. Mater.* **2020**, *244*, 118347. [[CrossRef](#)]
15. Cong, Z.; Jianxin, Z.; Jiahui, P.; Wenxiang, C.; Jiansen, L. Physical and Mechanical Properties of Gypsum-Based Composites Reinforced with Pva and Pp Fibers. *Constr. Build. Mater.* **2018**, *163*, 695–705. [[CrossRef](#)]
16. Adeyemi, A. Performance of cementitious composites reinforced with chopped basalt fibres—An overview. *Constr. Build. Mater.* **2021**, *266 Pt A*, 120970. [[CrossRef](#)]

17. Li, X.; Yu, T.; Park, S.; Kim, Y. Reinforcing Effects of Gypsum Composite with Basalt Fiber and Diatomite for Improvement of High-Temperature Endurance. *Constr. Build. Mater.* **2022**, *325*, 126762. [[CrossRef](#)]
18. Li, Z.; Wang, X.; Yan, W.; Ding, L.; Liu, J.; Wu, Z.; Huang, H. Physical and Mechanical Properties of Gypsum-Based Composites Reinforced with Basalt, Glass, and Pva Fibers. *J. Build. Eng.* **2023**, *64*, 695–705. [[CrossRef](#)]
19. Li, Z.; Wang, X.; Zhu, Z.; Wu, Z. Effect of Mixing Methods On the Dispersion of Fibers in the Gypsum Matrix and Performance Improvement Mechanism. *Constr. Build. Mater.* **2022**, *320*, 126193. [[CrossRef](#)]
20. Xie, L.; Zhou, Y.S.; Luo, S.; Fu, R.B.; Kong, D.W.; Wang, L.L. Study on Basalt Fiber Modified Desulfurized Building Gypsum. *Non-Met. Mines* **2020**, *43*, 49–51.
21. Wu, L.; Zhao, Z.M.; Zhu, w.m.; Luan, Y.; Wu, B. Effect of Chopped Basalt Fiber on the Bending Strength of Phosphogypsum. *Non-Met. Mines* **2017**, *40*, 9–11.
22. GB/T 17669.4-1999.1999-02-08; Gypsum Plasters—Determination of Physical Properties of Pure Paste. State Bureau of Building Materials Industry: Beijing, China, 1999.
23. Wu, L.; Zhao, Z.M.; Tian, R.; Quan, S.C.; Liu, Y.; He, J.Y.; Wu, B.; Dai, H.J. Orthogonal Test of Modified Phosphogypsum by Polypropylene Fibers and Polyvinyl Alcohol. *Bull. Chin. Ceram. Soc.* **2018**, *37*, 4022–4026. [[CrossRef](#)]

Disclaimer/Publisher’s Note: The statements, opinions and data contained in all publications are solely those of the individual author(s) and contributor(s) and not of MDPI and/or the editor(s). MDPI and/or the editor(s) disclaim responsibility for any injury to people or property resulting from any ideas, methods, instructions or products referred to in the content.